An experimental (digital photoelastic experiments) and numeric study of the stress field in the vicinity of two interacting cracks: stress intensity factors, T-stresses and coefficients of higher order terms

L.V. Stepanova[1]

[1]Samara National Research University, Moskovskoe Shosse 34A, Samara, Russia, 443086

Abstract. The multi-parameter description of the stress field in the neighbourhood of the crack tips of two interacting crack based on the photoelastic study and finite element analyses is given. Digital photoelasticity method is used for obtaining the isochromatic and isoclinic patterns in the plate with two collinear horizontal and two inclined cracks in anisotropic linear elastic material. Stress intensity factors, T-stresses and coefficients of the higher order terms in the multi-parameter Williams series expansion are experimentally determined. The finite element analysis for the cracked plates with the same configurations has been performed. Stress intensity factors, T-stress and coefficients of nine-term asymptotic expansion for the stress field are numerically obtained and are compared with the experimental results. The comparison shows good agreement of experimental and numerical estimations of these fracture mechanics parameters. Very good agreement is shown to exist between the digital photoelasticity method and finite element results confirming the effectiveness of the photoelasticity technique in obtaining the coefficients of higher order terms of the Williams series expansion from the experimental stress field around the crack tip.

1. Introduction

Photomechanics is an interdisciplinary research area applying optical measurement techniques to study mechanical behaviour of materials and structures [1-17]. Photoelasticity is an optical, non-contact technique used for whole field stress analysis which provides the information of principal stress difference (isochromatic) and principal stress direction (isoclinic) in the form of fringe contours. In the early days of its development, quantitative isoclinic and isochromatic data were obtained only along the fringe contours. With the advent of personal computer-based digital image processing systems, automation of photoelastic parameter estimation has now become popular and is often referred as digital photoelasticity [2,3]. Nowadays digital photoelasticity is effectively employed for obtaining the multi-parameter stress field description in the vicinity of the crack tip in isotropic elastic materials [1-17].

This work uses photoelastic techniques to investigate the effect of the influence of higher order terms on the crack tip stress field description. The aim of this paper is to obtain the coefficients of the higher-order terms in the Williams expansion and to estimate the influence of these terms on the stress field description taking into account as many as possible terms in the asymptotic presentation of the crack tip fields.

2. Experimental work: photoelastic experiments using plates with two horizontal collinear cracks and two inclined interacting cracks

All the specimens tested in this work were made by casting of polycarbonate. Plates with two collinear horizontal cracks and two inclined cracks were machined from the sheet to get the test specimens. Material properties of the photoelastic material are Young's modulus $E = 3GPa$, Poisson's ration $\nu = 0.3$ and the material fringe constant is found to be $f_\sigma = 18.38Pa\ m\ /\ fringe$. The plates with two horizontal collinear cracks under different loads are shown in Fig.1. The study uses a Java application programmed for the advanced determination of the fracture characteristics: coefficients of the Williams series expansion (WE) for the stress field in the vicinity of the crack tip. The skeleton of the fringe is identified first to accurately collect the data from the fringes. Global fringe thinning algorithm proposed by Ramesh and Promond [16] which uses the intensity information for the location of the fringe skeleton that is demonstrated to be the best methodology for fringe thinning [13]. The developed tool allows us to collect experimental points from the photoelasticity tests on the cracked specimens. An automatic routine implemented as a Java application permits to determine the values of coefficients of higher order terms of the WE that describe crack-tip fields (figures 1, e,f). Figures 2 and 3 show examples of fringe patterns for two inclined cracks under different loads.

The whole field fringe order and isoclinic values surrounding the crack tip are required to estimate the crack tip SIF, T-stresses and the coefficients of the higher-order terms in the Williams series expansion for the crack-tip stress field.

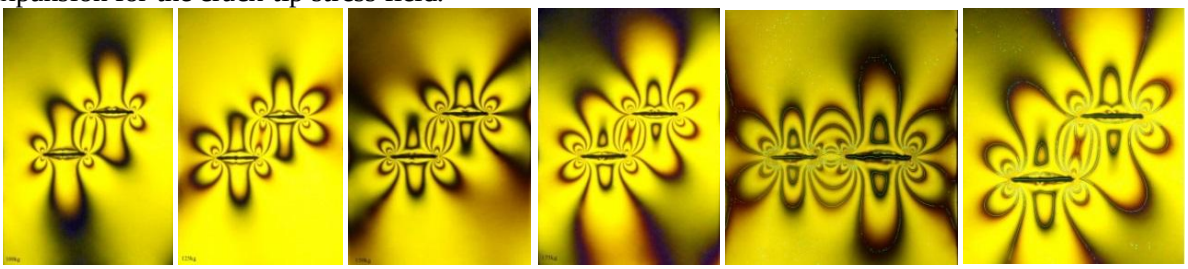

a) b) c) d) e) f)

Figure 1. Experimental specimens tested: isochromatic fringe pattern of the plate with two collinear horizontal cracks under different loads (a-d), skeleton of the fringe pattern (fringe thinned image) (e, f).

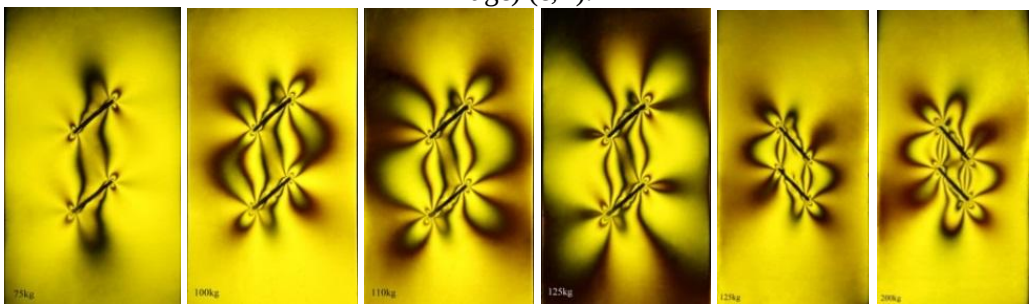

Figure 2. Isochromatic fringe pattern of the plate with two collinear inclined cracks under different loads.

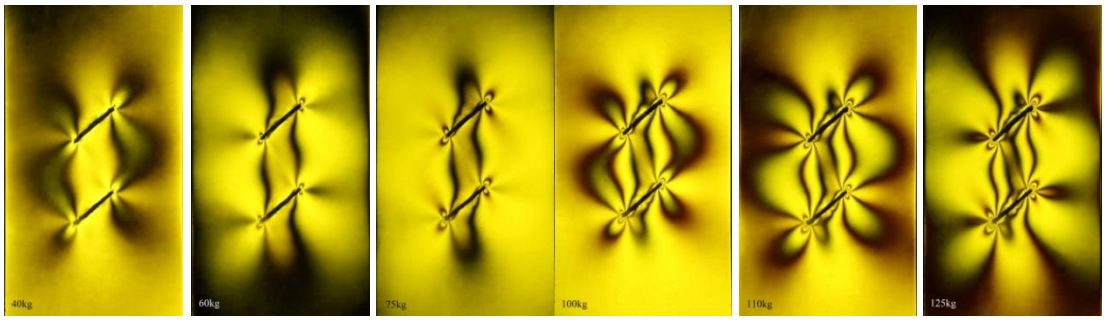

Figure 3. Isochromatic fringe pattern of the plate with two collinear inclined cracks under different loads.

3. Least-squares evaluation of SIFs, T-stresses and coefficients of higher-order terms

Williams [18] had derived crack tip stress field equations in polar coordinates for mixed mode loading. The stress field equations are given as

$$\sigma_{ij}(r,\theta) = \sum_{m=1}^{2} \sum_{k=-\infty}^{\infty} a_k^m r^{k/2-1} f_{m,ij}^{(k)}(\theta)$$

or in the expanded form

$$\begin{Bmatrix} \sigma_{11} \\ \sigma_{22} \\ \sigma_{12} \end{Bmatrix} = \sum_{n=1}^{\infty} \frac{n}{2} a_{In} r^{(n-2)/2} \begin{Bmatrix} \left(2 + n/2 + (-1)^n\right)\cos\left(n/2-1\right)\theta - (n/2-1)\cos(n/2-3)\theta \\ \left(2 - n/2 - (-1)^n\right)\cos\left(n/2-1\right)\theta + (n/2-1)\cos(n/2-3)\theta \\ (n/2-1)\sin\left(n/2-3\right)\theta - \left[n/2 + (-1)^n\right]\sin(n/2-1)\theta \end{Bmatrix} +$$
$$+ \sum_{n=1}^{\infty} \frac{n}{2} a_{IIn} r^{(n-2)/2} \begin{Bmatrix} \left(2 + n/2 - (-1)^n\right)\sin\left(n/2-1\right)\theta - (n/2-1)\sin(n/2-3)\theta \\ \left(2 - n/2 + (-1)^n\right)\sin\left(n/2-1\right)\theta + (n/2-1)\sin(n/2-3)\theta \\ -\left(n/2-1\right)\cos\left(n/2-3\right)\theta - \left[-n/2 + (-1)^n\right]\mathrm{co}(n/2-1)\theta \end{Bmatrix} \quad (1)$$

The coefficients are the unknown mode I and mode II parameters respectively. The SIFs can be computed from the coefficients as $K_I = a_{I1}\sqrt{2\pi}$, $K_{II} = -a_{II1}\sqrt{2\pi}$. The coefficient a_{I2} is related to T-stress as $\sigma_{0x} = T = -4a_{I2}$. The stress optic law relates the fringe order N and the in-plane principal stresses σ_I and σ_{II} as

$$Nf_\sigma / h = \sigma_1 - \sigma_2 \quad (2)$$

where is the material stress fringe value and is the thickness of the specimen. For a plane stress problem, the stress components are related to the principal stresses as

$$\sigma_1, \sigma_2 = (\sigma_{11} + \sigma_{22})/2 \pm \sqrt{(\sigma_{11} - \sigma_{22})^2/4 + \sigma_{12}^2}. \quad (3)$$

Substituting Eq. (3) in (2) one can define an error function for the data point:

$$g_m = \left((\sigma_{11} - \sigma_{22})/2\right)_m^2 + (\sigma_{12})_m^2 - \left((N_m f_\sigma)/(2h)\right)^2. \quad (4)$$

Eq. (4) is a non-linear equation in terms of the unknown parameters a_{Ij}, a_{IIj}. Initial estimates are made for these unknown parameters and substituted in Eq. (4) and possibly the error will not be zero since the estimates are not accurate [4, 12]. The estimates are then corrected using an iterative process based on Taylor series expansion of g_m. Finally, one can arrive at the solution of the incremental change by solving a simple matrix problem.

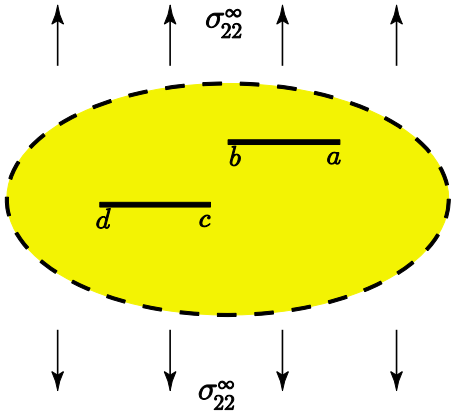

Figure 4. Schematic presentation of two horizontal cracks in the plate under tensile load.

The results of calculations are presented in Tables 1-4.

Table 1. The coefficients of the Williams series expansion for the stress field in the vicinity of the crack tip $z = a$.

$a_1^1(cm^{-3/2})$	$a_2^1(cm^{-2})$	$a_3^1(cm^{-5/2})$	$a_5^1(cm^{-7/2})$	$a_7^1(cm^{-9/2})$	$a_9^1(cm^{-11/2})$	$a_{11}^1(cm^{-13/2})$	$a_{13}^1(cm^{-15/2})$	$a_{15}^1(cm^{-17/2})$
0.5139	-0.2500	0.2512	-0.0646	0.0330	-0.0208	0.0145	-0.0109	0.0086
$a_{17}^1(cm^{-19/2})$	$a_{19}^1(cm^{-21/2})$	$a_{21}^1(cm^{-23/2})$	$a_{23}^1(cm^{-25/2})$	$a_{25}^1(cm^{-27/2})$	$a_{27}^1(cm^{-29/2})$	$a_{29}^1(cm^{-31/2})$	$a_{31}^1(cm^{-33/2})$	$a_{33}^1(cm^{-35/2})$
-0.0069	0.0058	-0.0049	0.00426	-0.0037	0.0033	-0.0029	0.0026	-0.0024
$a_{35}^1(cm^{-37/2})$	$a_{37}^1(cm^{-39/2})$	$a_{39}^1(cm^{-41/2})$	$a_{41}^1(cm^{-43/2})$	$a_{43}^1(cm^{-45/2})$	$a_{45}^1(cm^{-47/2})$	$a_{47}^1(cm^{-49/2})$	$a_{49}^1(cm^{-51/2})$	$a_{51}^1(cm^{-53/2})$
0.0022	-0.0020	0.0018	-0.0017	0.0016	-0.00015	0.0014	-0.0013	0.0012

Table 2. The coefficients of the Williams series expansion for the stress field in the vicinity of the crack tip $z = b$.

$a_1^1(cm^{-3/2})$	$a_2^1(cm^{-2})$	$a_3^1(cm^{-5/2})$	$a_5^1(cm^{-7/2})$	$a_7^1(cm^{-9/2})$	$a_9^1(cm^{-11/2})$	$a_{11}^1(cm^{-13/2})$	$a_{13}^1(cm^{-15/2})$	$a_{15}^1(cm^{-17/2})$
0.52398	-0.25000	0.27936	-0.04384	0.04700	-0.00820	0.00234	-0.00279	0.001468
$a_{17}^1(cm^{-19/2})$	$a_{19}^1(cm^{-21/2})$	$a_{21}^1(cm^{-23/2})$	$a_{23}^1(cm^{-25/2})$	$a_{25}^1(cm^{-27/2})$	$a_{27}^1(cm^{-29/2})$	$a_{29}^1(cm^{-31/2})$	$a_{31}^1(cm^{-33/2})$	$a_{33}^1(cm^{-35/2})$
-0.00126	0.01027	-0.00068	0.00769	-0.00041	0.00603	-0.00027	0.00489	-0.00018
$a_{35}^1(cm^{-37/2})$	$a_{37}^1(cm^{-39/2})$	$a_{39}^1(cm^{-41/2})$	$a_{41}^1(cm^{-43/2})$	$a_{43}^1(cm^{-45/2})$	$a_{45}^1(cm^{-47/2})$	$a_{47}^1(cm^{-49/2})$	$a_{49}^1(cm^{-51/2})$	$a_{51}^1(cm^{-53/2})$
0.00407	-0.00013	0.00345	-0.00009	0.00298	-0.00007	0.00260	-0.00005	0.00230

Table 3. The coefficients of the Williams series expansion for the stress field in the vicinity of the crack tip $z = c$.

$a_1^1(cm^{-3/2})$	$a_2^1(cm^{-2})$	$a_3^1(cm^{-5/2})$	$a_5^1(cm^{-7/2})$	$a_7^1(cm^{-9/2})$	$a_9^1(cm^{-11/2})$	$a_{11}^1(cm^{-13/2})$	$a_{13}^1(cm^{-15/2})$	$a_{15}^1(cm^{-17/2})$
0.62576	-0.25000	0.20400	-0.03470	0.01181	-0.00499	0.00234	-0.00117	0.00061
$a_{17}^1(cm^{-19/2})$	$a_{19}^1(cm^{-21/2})$	$a_{21}^1(cm^{-23/2})$	$a_{23}^1(cm^{-25/2})$	$a_{25}^1(cm^{-27/2})$	$a_{27}^1(cm^{-29/2})$	$a_{29}^1(cm^{-31/2})$	$a_{31}^1(cm^{-33/2})$	$a_{33}^1(cm^{-35/2})$
-0.00033	0.00018	-0.00010	0.00005	-0.00003	0.00002	-0.00001	$0.733 \cdot 10^{-5}$	$-0.442 \cdot 10^{-}$

Table 4. The coefficients of the Williams series expansion for the stress field in the vicinity of the crack tip $z = d$.

$a_1^1(cm^{-3/2})$	$a_2^1(cm^{-2})$	$a_3^1(cm^{-5/2})$	$a_5^1(cm^{-7/2})$	$a_7^1(cm^{-9/2})$	$a_9^1(cm^{-11/2})$	$a_{11}^1(cm^{-13/2})$	$a_{13}^1(cm^{-15/2})$	$a_{15}^1(cm^{-17/2})$
0.52397	-0.25000	0.27937	-0.04384	0.04700	-0.00820	0.02343	-0.00279	0.014687
$a_{17}^1(cm^{-19/2})$	$a_{19}^1(cm^{-21/2})$	$a_{21}^1(cm^{-23/2})$	$a_{23}^1(cm^{-25/2})$	$a_{25}^1(cm^{-27/2})$	$a_{27}^1(cm^{-29/2})$	$a_{29}^1(cm^{-31/2})$	$a_{31}^1(cm^{-33/2})$	$a_{33}^1(cm^{-35/2})$
-0.00126	0.01027	-0.000068	0.00769	-0.00041	0.00603	-0.00026	0.00489	-0.00018
$a_{35}^1(cm^{-37/2})$	$a_{37}^1(cm^{-39/2})$	$a_{39}^1(cm^{-41/2})$	$a_{41}^1(cm^{-43/2})$	$a_{43}^1(cm^{-45/2})$	$a_{45}^1(cm^{-47/2})$	$a_{47}^1(cm^{-49/2})$	$a_{49}^1(cm^{-51/2})$	$a_{51}^1(cm^{-53/2})$
0.00407	-0.00013	0.00345	-0.00009	0.00298	-0.00007	0.00260	-0.00005	0.00230

4. Finite element analysis

The plates with two cracks used were modelled with 2D quadratic elements away from the crack tip. The crack neighbourhood is meshed with quarter point triangular elements. Figure 5 shows the meshed plate. Cracks are modelled as a seam in which the crack faces are free to move apart. Contour integral method available in SIMULIA ABAQUS software is employed to determine stress intensity

factors. Twenty contour integrals are used to extract the stress intensity factor values. The output for contour integral is obtained using a sweep mesh.

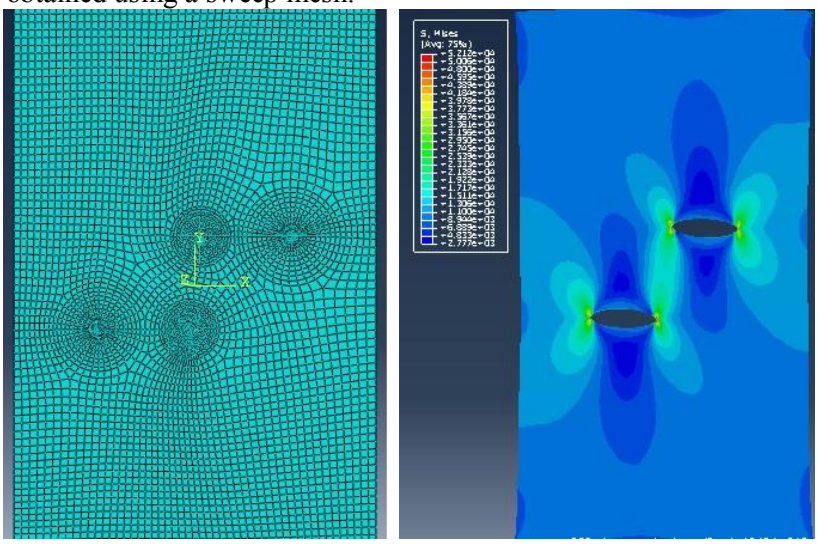

Figure 5. A meshed plate with two horizontal cracks and the von Mises equivalent stresses.

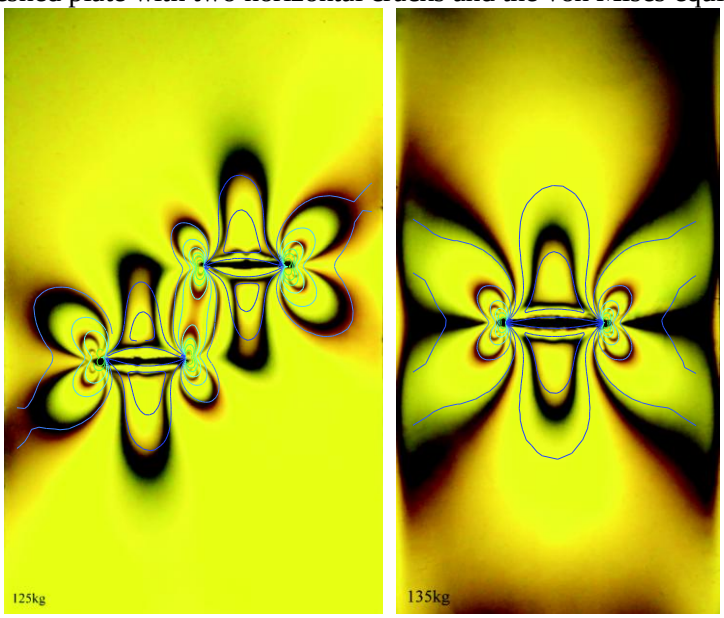

Figure 6. Theoretically constructed stress field based on the Williams series expansion shown by blue lines.

Figure 6 shows the theoretically reconstructed equivalent stress based on the multi-parameter description in the plate. The multi-parameter description is shown by blue lines.

5. Conclusions

Crack interaction effects at the crack tips of two horizontal collinear cracks and two inclined cracks are investigated by means of digital photoleasticity method and finite element method. The SIF values are evaluated with the help of digital image processing, the overdeterministic method and a nonlinear least squares method. The coefficients of the higher order terms are found. Very good agreement is shown to exist between the digital photoelasticity method and finite element results confirming the effectiveness of the photoelasticity technique in obtaining the coefficients of higher order terms of Williams series expansion from the experimental stress field around the crack tip.

In this research, photoelasticity is employed to assess the complete Williams series coefficients of the linear elastic stress field in the vicinity of the crack tip for a wide class of experimental specimens subject to mixed mode loading: plates with two collinear cracks under tensile loading, pure shear

loading and mixed mode loading. The study has showed that the coefficients of higher order terms can play an important role in fracture process in notched and cracked structures. The approach developed allows us to construct all the higher order terms in the asymptotic expansions in order to better approximate stress field. We use the plate with two collinear cracks under mixed mode loading to construct the complete multi-parameter asymptotic expansion of the stress field in the vicinity of the crack tip.

By means of photoelasticity the distribution of the isochromatic fridge patterns and the stress field near the crack tip based on the complete Williams asymptotic expansion for various classes of the experimental specimens under mixed mode loading are obtained. In the present contribution fracture mechanics problems regarding the study of the stress and displacement fields around a crack tip under mixed mode loading are discussed in the framework of photoelastic techniques and an over-deterministic method for calculation of the coefficients of crack tip asymptotic field. The comparison of the experimental results and the calculations performed with finite element analysis has shown the importance and significant advantages of photoelastic observations for the multiparametric description of the stress field in the neighbourhood of the crack tip. The study is aimed at experimental and computational determination of the coefficients in crack tip asymptotic expansions for a wide class of specimens under mixed mode loading conditions. In the paper multi-parametric presentation of the stress filed near the crack tips for a wide class of specimens is obtained. Theoretical, experimental and computational results obtained in this research show that the isochromatic fringes in the vicinity of the crack tip are described more accurately when we consider the complete Williams asymptotic expansion of the stress field and we have to keep the higher order stress terms in the asymptotic expansion since the contribution of the higher order stress terms (besides the stress intensity factors and the T-stress) is not negligible in the crack tip stress field. A good correlation was observed between the experimental results and the numerical results obtained from finite element analysis.

6. Acknowledgments

The reported study was funded by RFBR, project 19-01-00631.

7. References

[1] Ramesh, K. An improves normalization technique for white light photoelasticity / K. Ramesh, A. Pandey // Opt Lasers Eng. – 2018. – Vol. 109. – P. 7-16.

[2] Patil, P. Linear least squares approach for evaluating crack tip gracture parameters using isochromatic and isoclinic data from digital photoelasticity / P. Patil, C.P. Vyasarayani, M. Ramji // Optics and Lasers in Engineering. – 2017. – Vol. 93. – P. 182-194.

[3] Aytollahi, M.R. Experimental determination of stress field parameters in bi-material notches using photoelasticity / M.R. Aytollahi, M.M. Mirsayar, M. Dehghany // Materials and Design. – 2011. – Vol. 32. – P. 4901-4908.

[4] Hello, G. Derivation of complete crack-tip stress expansion from Westergaard-Sanford solutions // International Journal of Solids and Structures. – 2018. – Vol. 144-145. – P. 265-275.

[5] Hello, G. Analytical determination of coefficients in crack-tip stress expansions for a finite crack in an infinite plane medium / G. Hello, M.B. Tahar, J.-M. Roelandt // International Journal of Solids and Structures. – 2012. – Vol. 49. – P. 556-566.

[6] Ramesh, K. Evaluation of stress field parameters in fracture mechanics by photoelastisity-revisited / K. Ramesh, S. Gupta, A.A. Kelkar // Engineering Fracture Mechanics. – 1997. – Vol. 56. – P. 25-45.

[7] Stepanova, L.V. A Photoelastic Study for Multiparametric Analysis of the Near Crack Tip Stress Field Under Mixed Mode Loading / L.V. Stepanova, P.S. Roslyakov, P.N. Lomakov // Procedia Structural Integrity. – 2016. – Vol. 2. – P. 1797-1804.

[8] Pisarev, V.S. Combining the crack compliance method and speckle interferometry data for determination of stress intensity factors and T-stress / V.S. Pisarev, Y.G. Matvienko, S.I. Eleonsky, I.N. Odintsev // Engineering Fracture Mechanics. – 2017. – Vol. 179. – P. 348-374.

[9] Magalhaes junior, P.A.A. Computational method of phase shifting to stress measurement with photoelasticity using plane polariscope / P.A.A. Magalhaes junior, C.A. Magalhaes, A.L.M.A. Magalhaes // Optic. – 2017. – Vol. 130. – P. 213-226.
[10] Brinez, J.C. Computational hybrid phase shifting technique applied to digital photoelasticity / J.C. Brinez, A.R. Martinez, J.W. Branch // Optik. – 2018. – Vol. 157. – P. 287-297.
[11] Ramakrishnan, V. Scanning schemes in white light photoelasticity. Part II: Novel fringe resolution guided scanning scheme / V. Ramakrishnan, K. Ramesh // Optics and Lasers in Engineering. – 2017. – Vol. 92. – P. 141-149.
[12] Vasco-Olmo, J.M. Investigation of effective stress intensity factors during overload fatigue cycles using photoelastic and DIC techniques / J.M. Vasco-Olmo, B.Yang, M.N. James, F.A. Diaz, Theoretical and Applied Fracture Mechanics. – 2018. – Vol. 97. – P. 73-86.
[13] Vivekanandan, A. Study of interaction effects of asymmetric cracks under biaxial loading using digital photoelasticity / A. Vivekanandan, K. Ramesh // Theoretical and Applied Fracture Mechanics. – 2019. – Vol. 99. – P. 104-117.
[14] Fernandez, M.S.-B. Evaluation of uncertainty in the measurement of the crack-tip stress field using photoelasticity // The Journal of Strain Analysis for Engineering Design. – 2019. – Vol. 54. – P. 24-35.
[15] Stepanova, L. Interference-optical methods in mechanics for the multi-parameter description of the stress fields in the vicinity of the crack tip / L.V. Stepanova, V.S. Dolgikh // Journal of Physics: Conference Series. – 2018. – Vol. 1096. – P. 012117.
[16] Stepanova, L.V. Asymptotic analysis of the crack tip stress field (Consideration of higher order terms) // Numerical Analysis and Applications. – 2019. – Vol. 12(3). – P. 284-296.
[17] Jobin, T.M. Experimental of the strain intensity factor at the inclusion tip using digital elasticity / T.M. Jobin, S.N. Khanderi, M. Ramji // Optics and Lasers in Engineering. – 2020. – Vol. 126. – P. 105855.
[18] Williams, M.L. Stress singularities resulting from various boundary conditions in angular corners of plates in tension // Journal of Applied Mechanics. – 1952. – Vol. 19. – P. 109-114.